A Study on the Retrieval Algorithms for Atmospheric Parameters from FORMOSAT-3/COSMIC Occultation Data

Wen-Hao Yeh[1], Tsen-Chieh Chiu[2], Cheng-Yung Huang[3], Yuei-An Liou[1,4]

[1] Center for Space and Remote Sensing Research, NCU, Taiwan
[2]Department of Electrical Engineering, NCU, Taiwan
[3]National Space Organization, Taiwan
[4]Institute of Space Science, NCU, Taiwan

ABSTRACT

Radio occultation technique has been used in planetary science to obtain reliable and accurate temperature profiles of the other planets' atmosphere for decades. It relies on the fact that radio waves are bent and delayed due to the gradient of atmospheric refractivity along-ray-path. With the advent of Global Positioning System (GPS), it becomes possible to retrieve the refractivity and temperature profiles of the Earth's atmosphere from the occultation data.

We have developed a retrieval algorithm and compared the results of our algorithm with the data of CHAMP to verify the accuracy of our algorithm is good enough. In our algorithm, there are some smoothing steps when retrieving. We analysis the data of FORMOSAT-3 and compare the results with and without smoothing and the results of TACC to see is there any phenomenon deleted after smoothing.

KEY WORDS: GPS, FORMOSAT-3, CHAMP, TACC

1. INTRODUCTION

Radio occultation (RO) technique has been used to observe planetary atmosphere for more than thirty years (Fjeldbo et al., 1971 and Tyler, 1987) since NASA begin to explore planets in solar system. With the Global Positioning System (GPS) has been built up, a lower earth orbit (LEO) satellite MicroLab-1 launched to receive GPS signal to observe atmosphere parameters and distribution of electron density in ionosphere (Ware et al. 1996). This mission verified that it is workable to get atmosphere parameters by using LEO to do RO observation. Thus, there are many proposal of RO observation has been brought up, like Oersted (Escudero et al., 2001), SUNSAT (Mostert and Koekemoer, 1997), CHAMP (Wickert et al., 2001), and SAC-C. In April 2006, FORMOSAT-3 has been launched. Presently, we can get more than 1500 RO data from FORMOSAT-3 satellites and 300-400 RO data per day for us to develop our retrieval technique.

RO technique use LEO satellites to receive the two frequency signal from GPS satellites. When signal go through atmosphere, the medium in atmosphere makes signal delay and its refraction index gradient curved the path of signal. RO technique is using the delay of GPS signal and the position of GPS and LEO satellites to retrieve atmosphere parameters and distribution of electron density.

In this paper, we will compare our result with UCAR and then determine the influence of smoothing step in retrieval process.

2. COMPARISON BETWEEN NCURO & UCAR

We have follow the procedure of UCAR CDAAC RO data processing and form an processing procedure, named NCURO, to retrieve excess phase to bending angle, pressure, and temperature profile of atmosphere. The UCAR CDAAC RO data processing procedures are shown in Figure 1.

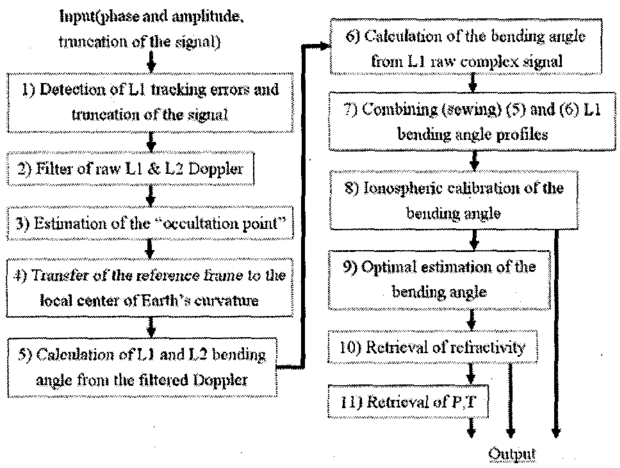

Figure 1. Flow diagram of the UCAR CDAAC RO data processing procedures. (Kuo Y. H., et al., 2004)

We retrieved the data of GPSMET and CHAMP and form the temperature profile of atmosphere. NCURO can retrieve the data which UCAR can retrieve. Presently, NCURO can retrieve more than half RO data. The results of some cases are shown in Figure 2. In Figure 2, the red and black lines are the temperature profile of atmosphere retrieved by NCURO and UCAR of GPSMET and CHAMP RO data. For the most part of results retrieved by NCURO are more than retrieved by UCAR, but the breadth is very few.

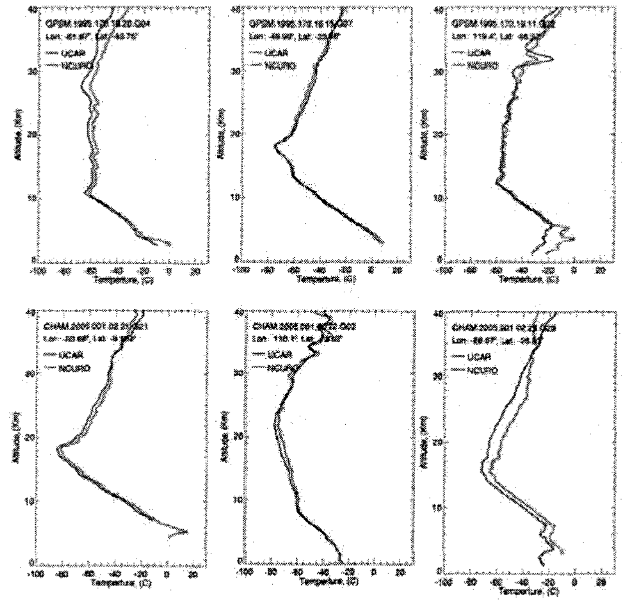

Figure 2. Red: NCURO; Black: UCAR. **Up:** The retrieval results of GPSMET by using L1 and L2. **Down:** The retrieval results of CHAMP by using L1.

3. SIGNAL SMOOTHING MODEL

3.1 Signal Smoothing Principle

NCURO follow the procedures in Figure 1. In the fifth step in Figure 1, NCURO has a smoothing process after calculate the bending angle of L1 and L2. The smoothing method follow the Constrained Matrix Smoothing Method (CMSM), brought up by D.D. Feng and B.M. Herman in 1999. The mathematical form of CMSM is

$$\vec{f}_s(t_1,t_2,\cdots,t_n)=\left[\bar{I}+\bar{S}^T\bar{\Gamma}\bar{S}\right]^{-1}\times\vec{f}_d(t_1,t_2,\cdots,t_n) \quad (1)$$

where $\vec{f}_s$ is the Doppler shift after smoothing,

$\vec{f}_d$ is the raw Doppler shift,

I is unit matrix,

Γ is weighting matrix.

The form of matrix $\bar{S}$ is

$$\bar{S}=\begin{vmatrix} 0 & 0 & 0 & 0 & 0 & 0 & 0 \\ -1 & 2 & -1 & 0 & 0 & 0 & 0 \\ 1 & -3 & 3 & -1 & 0 & 0 & 0 \\ 0 & 1 & -3 & 3 & -1 & 0 & 0 \\ 0 & 0 & 1 & -3 & 3 & -1 & 0 \\ 0 & 0 & 0 & 1 & -3 & 3 & -1 \\ 0 & 0 & 0 & 0 & -1 & 2 & -1 \end{vmatrix}. \quad (2)$$

The retrieved result of one case of CHAMP RO data is shown in Figure 3. The result with smoothing is on left, and without smoothing is on right. It is obviously that the unsmooth part of bending angle is mostly under the altitude of 10 km and the reason is conjectured that the moisture almost distributes near the earth surface and fluctuate the signal.

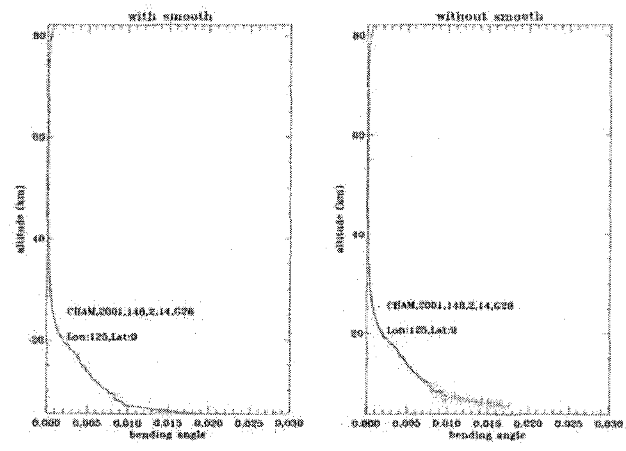

Figure 3. Left: Bending angle with smooth. **Right:** Bending angle without smooth.

3.2 Analysis of CHAMP data

We analyzed the data of CHAMP from May to December, 2001, and from E118°～144°, N4°～46°. The diagram is shown in Figure 4. We separated this area in six parts. Then gathered the RO data and get the results and difference with and without smoothing of bending angle of each data in each part.

Thus, we can get the mean difference between analyze with and without smoothing in this period. The results are shown in Figure 5. In Figure 5, the large difference parts are all under the altitude of 10km. The maximum difference of area 1, area 3, and area 6 are less than other three areas. In Figure 4 we can see that the ratio of land and ocean in area1, area3, and area 6 are more than other three areas. It is conjectured that the moisture above ocean is more than above land, so the fluctuation of signal is larger above ocean is larger than above land.

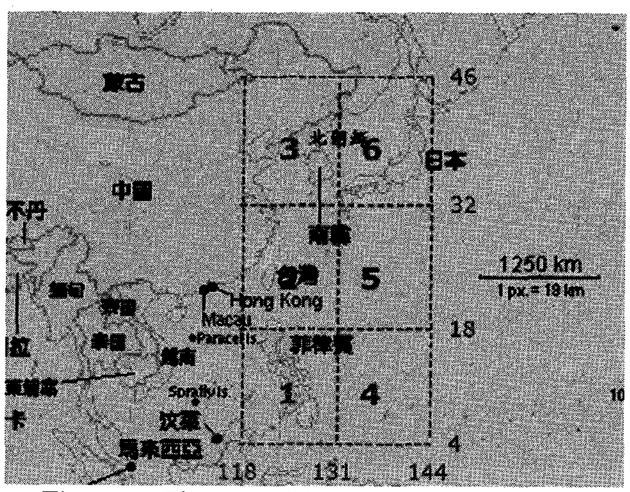

Figure 4. The area which we have analyzed the data of CHAMP. The numbers in the right and below are the latitude and longitude.

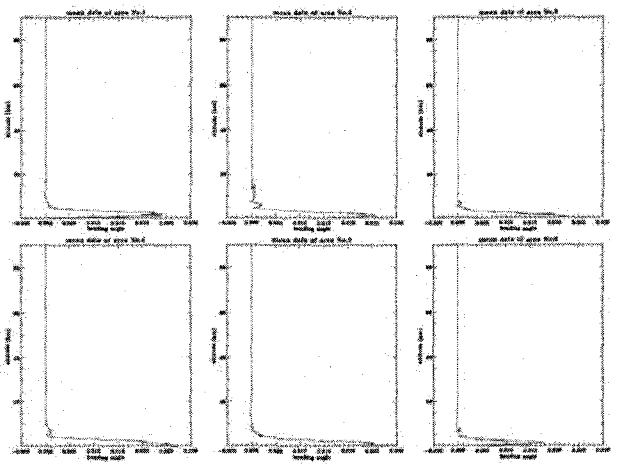

Figure 5. The mean difference of bending angle between analyze with and without smoothing.

3.3 Comparison with Radiosonde

Because of the bad quality in L2 of CHAMP, we used the data of GPSMET to do ionosphere correction. We followed the ionosphere correction method brought up by Vorob'es and Krasil'nikova in 1994, and the mathematic form is:

$$\alpha(a)=\frac{f_1^{\,2}\alpha_1(a)-f_2^{\,2}\alpha_2(a)}{f_1^{\,2}-f_2^{\,2}} \qquad (3)$$

where a is impact parameter,

$\alpha_1(a)$ is the bending angle of L1,

$\alpha_2(a)$ is the bending angle of L2.

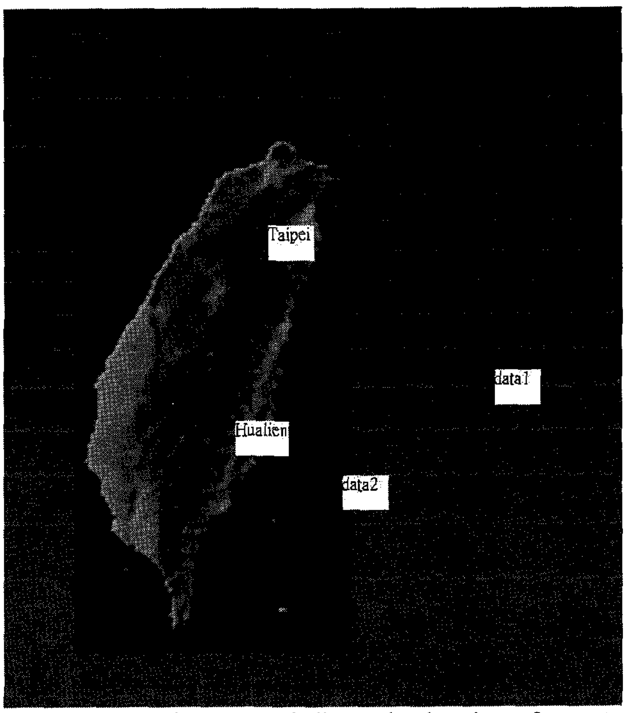

Figure 6. The arrows indicate the location of two radiosonde stations and the location of two RO data. Data1 is used to compare with Taipei radiosonde station and data2 is used to compare with Hualien radiosonde station.

There are two radiosonde stations in Taiwan. One is in Taipei and the other is in Hualien. Radiosonde launched in 8:00AM and 8:00PM every day. The time and location of RO data cannot match radiosonde launch time. So we only consider the location and neglect the time of RO data to match radiosonde. The time of two RO data we took to do comparison are at 2:00PM and 6:00PM to do comparison with radiosonde data in Taipei and Hualien in 8:00PM.

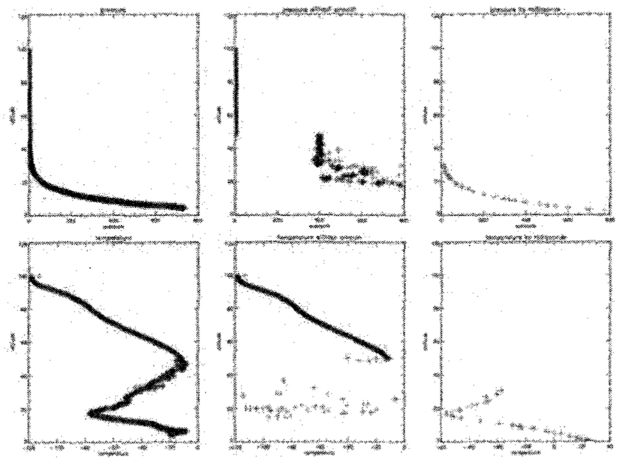

Figure 7. The retrieval results of RO data and Taipei radiosonde data. **Up:** Pressure; **Down:** Temperature; **Left:** Analyze with smooth; **Middle:** Analyze without smooth; **Right:** The data of radiosonde.

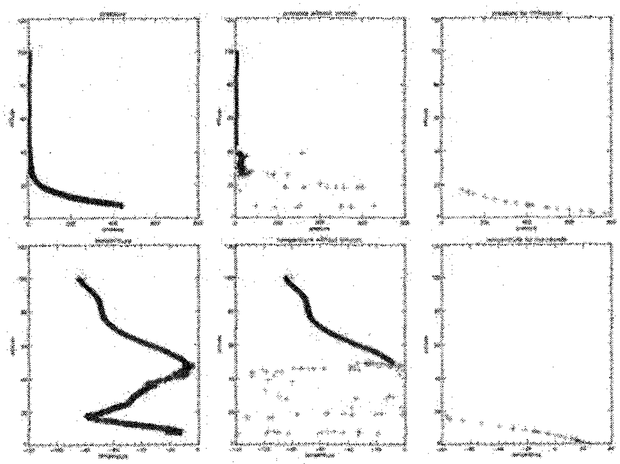

Figure 8. The retrieval results of RO data and Hualien radiosonde data. **Up:** Pressure; **Down:** Temperature; **Left:** Analyze with smooth; **Middle:** Analyze without smooth; **Right:** The data of radiosonde.

The relative location of two radiosonde stations and the location of two RO data is shown in Figure 6. The arrows indicate the location of two radiosonde stations and the location of two RO data. Data1 is used to compare with the data of Taipei radiosonde station and data2 is used to compare with the data of Hualien radiosonde station. The comparison results are shown in Figure 7 and Figure 8.

Because of the limit of observing altitude of radiosonde, the highest data point of two radiosonde data are 17km and 10km. In Figure 7 and Figure 8, the pressure and temperature of RO data with smoothing and radiosonde data conforms each other. It prove again that NCURO is usable to analyze RO data.

3.4 Analysis of FORMOSAT-3 data

FORMOSAT-3 satellites, the different from other RO satellites, install open loop (OL) instead of phase lock loop (PLL) to catch phase when the altitude of RO point under about 10km. GPS satellites send wave pattern and code and the signal structure is shown in Figure 9. GPS use PSK form to transport signal.

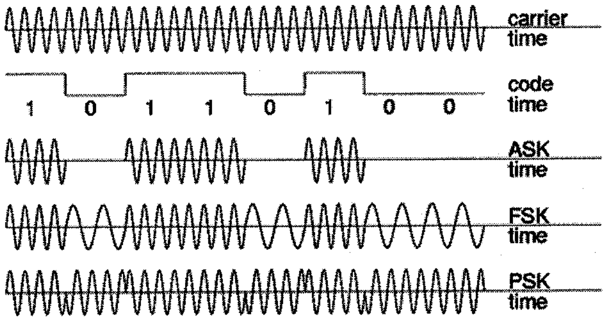

Figure 9. GPS signal structure. GPS use PSK form to transport signal.

In PLL, satellites can use former catch signal to get code of GPS signal and remove the effect of code. In OL, satellites not use former catch signal to catch wave but use a simulated signal, so it cannot remove the effect of code. In GPS wave pattern, phase changes 180° when code changes from 1 to 0 or 0 to 1. So excess phase jump up or down when code changes. The difference of excess phase change with time of one case is shown in Figure 10. It is obviously that there are three lines in the front of data. The period with triple line indicate the usage of OL. We have to combine these lines into one line, but we have no effective method presently. This is one of the future works of us.

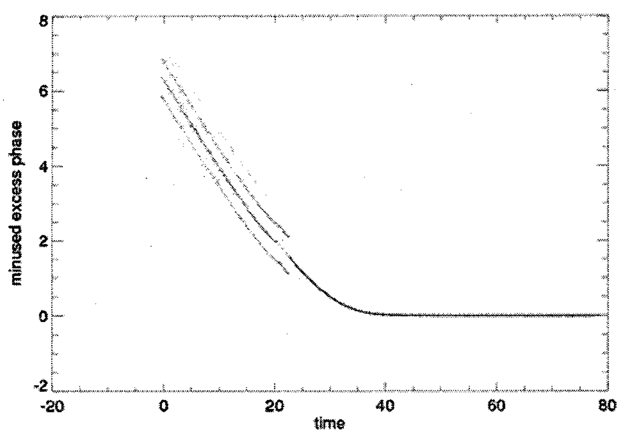

Figure 10. The difference of excess phase changes with time.

4. CONCLUSION

We use the data of CHAMP and GPSMET to test our algorithm and compare with the result of UCAR. It verifies our algorithm is usable. In section 3.2, analyzing unsmooth data can tell us something in atmosphere. In section 3.3, it is the most directly way to compare retrieval result and real atmosphere situation. In section 3.4, the effect of OL is considerable, and what we are proceeding is to develop an algorithm to remove the influence of OL.

5. REFERENCE

Escudero, A., Schlesier, A.C., Rius, A., Flores, A., Rubek, F., Larsen, G.B., Syndergaard, S., Hoeg, P., 2 Ionospheric tomography using Orsted GPS measurements—Preliminary results. *Physics and Chemistry of Earth*, A 26 (3), 173–176, 2001.

Feng D. D. and M. Herman, Remote Sensing the Earth's Atmosphere Using the Global positioning System (GPS) — The GPS/MET Data Analysis, *J. Atmos. Oceanic Technol.,* 16, 989, 1999

Kuo Y. H. , T.-K. Wee, S. Sokolovskiy, C. Rocken, W. Schreiner, D. Hunt, R. A. Anthes, Inversion and Error Estimation of GPS Radio Occultations, *JMSJ.*, Vol. 82, No.1B, pp. 507-531, 2004.

Mostert, S., Koekemoer, J.A., The science and engineering payloads and experiments on SUNSAT. *Acta Astronautica*, 41 (4 –10), 401–411, 1997.

Vorob'ev, V. V., and T. G. Krasil'nikova, Estimation of the accuracy of the atmospheric refractive index recovery from Doppler shift measurements at frequencies used in the NAVSTAR system, *Phys. Atmos. Ocean*, 29, 602-609, 1994.

Wickert, J., A. G. Pavelyev, Y. A. Liou, T. Schmidt, C. Reigber, K. Igarashi, A. A. Pavelyev, and S. Matyugov, Amplitude variations in the GPS signals as a possible indicator of inonspheic structures, *Geopsys. Res. Letters*, Vol. 31, L24801.